

# Wave energy converter farm feasibility assessment in southwest Baja California, Mexico

Alfredo Sánchez, Edgar Mendoza\*

*Institute of Engineering, National Autonomous University of Mexico, Mexico*

## ARTICLE INFO

### Keywords:

Marine renewable energy  
Wave energy converter  
WEC farm  
Levelized cost of energy

## ABSTRACT

This study evaluates the technical and economic feasibility of implementing a wave energy converter (WEC) farm on the southwest coast of Baja California, Mexico. The aim is to determine the theoretical installed capacity and the levelized cost of energy (LCOE) for a WEC farm, unlike most previous efforts that were limited to a single device. The availability of wave energy has been assessed using 40 years of wave data. The electrical power generation potential of the Archimedes Wave Swing and Wave Dragon devices was estimated using their power matrices. For the calculation of levelized cost of energy, the capital expenditure includes equity, debt, taxes, and the present value of the power generation over the project's lifespan. The results indicate that the Archimedes Wave Swing farms offer the most favourable pricing for end users, despite the Wave Dragon farms having a larger installed capacity. A sensitivity analysis was conducted for five variables, which revealed that site selection has the greatest impact on LCOE.

## 1. Introduction

The energy sector is facing a complex predicament. The demand for energy is rapidly increasing, but much of today's energy comes from sources that are nearing depletion or have unacceptable environmental impacts. Therefore, the implementation of cleaner and renewable energy sources, as well as low-environmental-footprint technologies, is crucial.

In order to meet commitments such as the Paris Agreement targets [1], the renewable energy industry must grow more rapidly. Promising energy sources for increasing installed capacity based on renewables include biomass and ocean energy. Ocean energy is an exciting and versatile alternative, due to the various forms of energy available, such as ocean currents, tides, waves, and thermal and salinity gradients.

Wave energy has a theoretical worldwide potential of 93,000 TWh [2]. The technologies for converting this energy source are rapidly advancing. Significant investment in device optimization has driven this growth, with several concepts already at the pilot plant stage. Some of these pilot plants are now close to begin commercial operation, with the aim of improving electricity distribution.

In parallel with the development of the technology, the economic aspects need to be addressed in order to attract investors for the deployment of wave energy power plants. This requires estimating the

possible installed capacity of plants in specific locations, as well as the costs of energy, as the minimum information required for decision making. However, in order for the figures to be as accurate as possible, estimations must be conducted based on a group of devices occupying a delimited marine area, also known as farm.

Although there are several assessments that evaluate the economic performance of individual devices [3–6], limited research has been conducted on the feasibility of entire energy farms [7]. That is, no prior research has considered together the spatial distribution of available wave energy for determining the optimal deployment site and the power damping across the lines of devices within the farm. Such an approach should result in a more accurate estimation of output power and energy costs.

The purpose of this research is to assess the feasibility of an entire wave energy converter (WEC) farm. The study also presents a technique for computing the levelized cost of energy for WEC farms. Two well-known devices were selected for the farms: the Archimedes Wave Swing and the Wave Dragon. The study used small-scale wave numerical modelling to calculate the power available for each device on the farm, considering the natural distribution caused by the bathymetry and the damping caused by the devices' lines. A sensitivity analysis was performed to provide an overview of the impact of certain variables on the cost of energy.

The article commences by outlining the LCOE methods used and the

\* Corresponding author. Circuito exterior S/N, Instituto de Ingeniería, edificio, 17, cub. 209, Ciudad Universitaria, Coyoacan, 04510, Mexico.  
E-mail address: [emendozab@ingen.unam.mx](mailto:emendozab@ingen.unam.mx) (E. Mendoza).

Nomenclature			
$CF$	Plant capacity factor	$P_{ij}$	Sea state probability of occurrence
$D_y$	Distance between devices	$P_N$	Line number
$E$	Yearly theoretical wave energy	$P_w$	Theoretical wave power
$E_{max}$	Maximum power produced in a year	$Q_{ij}$	Theoretical power matrix
$E_{prod}$	Annual power produced	$Q_t$	Net electric generation along the period t
$F_d$	Debt financing	$R_F$	Risk-free rate
$F_p$	Equity financing	$R_I$	Return rate
$H_s$	Significant wave height	$R_M$	Stock market rate of return
$K_{TD}$	Transmission coefficient of a single device	$R_p$	Country risk bonus
$L_{tot}$	Total length of the farm	$t$	Yearly hours
$L_p$	Deep water wave length	$T_{an}$	Annual rate
$L_x$	Device length parallel to the wave fronts	$T_{int}$	Interest rate at which the debt was contracted
$L_y$	Length of the device perpendicular to wave fronts	$T_m$	Mean wave period
$LCC$	Levelized capacity charge	$T_{men}$	Monthly rate
$LCOE$	Levelized cost of energy	$T_p$	Peak wave period
$n_H$	Number of wave height classes	$VPC$	Present value of the electric plant costs
$n_T$	Number of wave period classes	$WACC$	Weighted average capital cost
$N_{DN}$	Number of devices in line N	$\beta_i$	Company specific risk indicator
$N_{GN}$	Number of gaps in line N	$\theta$	Wave direction
		$\rho$	Water density

WEC devices considered, along with their power matrices in Section 2. The study site and numerical model characteristics are also presented. Section 3 displays the outcomes achieved from the WEC farm deployment and LCOE estimation. In Section 4, the findings are debated through a comparative analysis of the chosen WECs. The primary conclusions are outlined in Section 5.

## 2. Methods

The methodology presented here considers the energy distribution and the energy attenuation due to the array together for the energy cost calculation. Efforts have been made for the former and the latter [8,9], but not together. The methodology followed can be summarized as follows (see Fig. 1):

The initial step involves selecting the study site and evaluating waves at the chosen points through statistical analysis. The objective is to

identify the optimal point for wave propagation. Using the information gathered, wave propagation modelling towards the coast was conducted using the WAPO numerical tool. The modelling results enabled the identification of the area within the study site with the highest available power. Polygons of 1.12 km<sup>2</sup> are proposed to determine the location of the WEC farm based on their compatibility with the study site and the information available. The WECs are distributed accordingly. The maximum power generation of each farm is evaluated, considering the losses due to the interaction of the WEC array with the waves.

The most energetic polygon for each type of WEC is identified, and the annual generation time and expected energy output per year are estimated using energy thresholds. A detailed financial analysis is then performed, considering aspects such as equity, debt, and taxes, to calculate the levelized cost of energy (LCOE) for each proposed farm.

The following sections describe the methodology shown in Fig. 1.

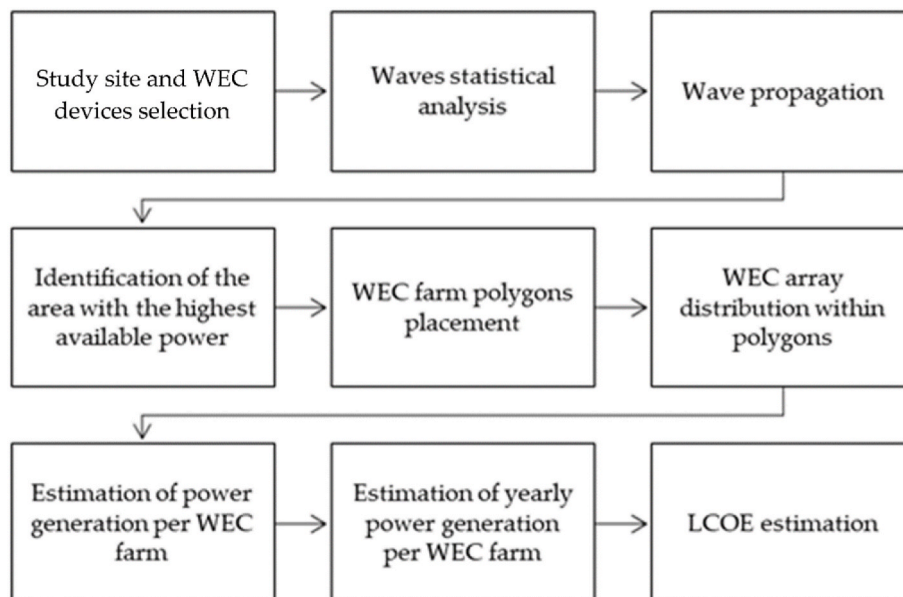


Fig. 1. Proposed methodology.

2.1. Study site and devices selection

2.1.1. Study site

Mexico is geographically well-positioned for wave power availability, with 11,500 km of coastline, it is one of the countries with longest coastlines in the world [10]. The coastal regions of Mexico have abundant energy resources, facing the world's two major oceans. However, it is known that the north Pacific coast has the largest available power (~20 kW/m). The exploitation of these resources could significantly benefit the coastal communities. Nevertheless, the inclusion of this energy source in the Mexican power matrix is still pending.

Todos Santos Bay is located on the northwest coast of the Baja California peninsula, between 31° 40' and 31° 56' north latitude and 116° 36' and 116° 5' west longitude (see Fig. 2). Its natural boundaries give it a trapezoidal shape, with approximately 24,090 ha, 18 km in length and 15 km in width.

This bay was selected as a case study due to its favourable wave conditions for the installation of WEC devices. Ensenada, the largest city in this bay is Ensenada, is a coastal city that attracts millions of tourists annually, highlighting its economic significance [11].

2.1.2. Description of the devices under study

Wave Dragon.

This overtopping WEC has a rated output of between 4 and 11 MW, depending on its size and location (Fig. 3).

In general, the main characteristics of the Wave Dragon are.

- Two reflectors attached to the main structure, which direct the waves towards the device's reservoir.
- The main structure consists of a double curved ramp and a water reservoir.
- Hydraulic turbines are used to convert hydraulic energy into electrical energy.

The Wave Dragon prototype, measuring 27 × 37 m, has been tested since the beginning of the 21st century in the Nissum Bredning lagoon in Denmark. The Wave Dragon website states that it was the world's first grid-connected WEC [13]. Table 1 displays the main characteristics of the three available models.

The power matrix of this device is shown in Fig. 4, where Hs stands for significant wave height and Tm is the mean wave period.

The power matrix of the Wave Dragon (Fig. 4) reveals that its best performance occurs for significant waves higher than 4 m for periods between 4 and 12 s.

2.1.2.1. Archimedes Wave Swing. This point absorber has a rated power of 2 MW. It was tested in 2004 in Póvoa de Varzim, Portugal, in a pilot

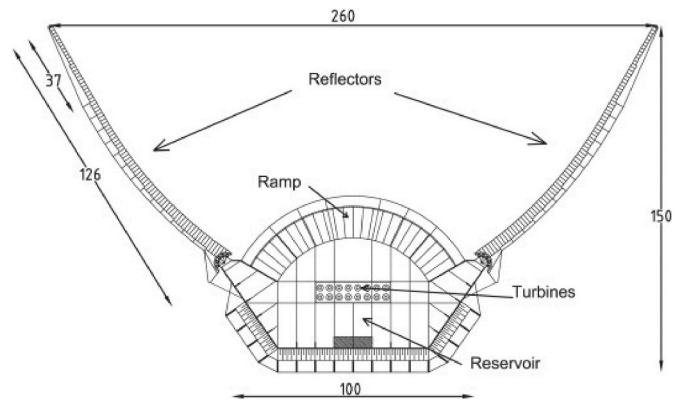


Fig. 3. Wave Dragon structure [12].

Table 1  
Main characteristics of Wave Dragon [13].

	MODEL 1	MODEL 2	MODEL 3
TOTAL WEIGHT [TON]	22,000	33,000	54,000
SIZE [M]	260 x 150	300 x 170	390 x 220
NOMINAL POWER [MW]	4	7	11
WATER DEPTH [M]	>20	>25	>30

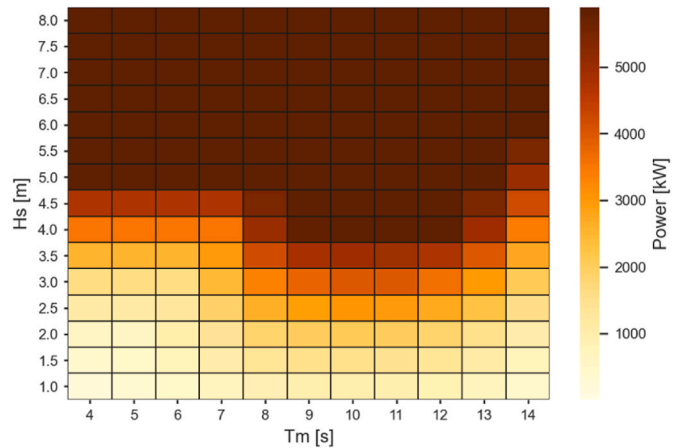


Fig. 4. Wave Dragon power matrix [14].



Fig. 2. Todos santos bay, baja California, Mexico.



Fig. 5. Archimedes Wave Swing pilot plant [15].

plant designed by Teamwork Technology BV in collaboration with private companies and research institutes [15]. Fig. 5 shows the pilot plant.

Table 2 provides a general overview of Archimedes Wave Swing key features.

Fig. 6 shows the performance matrix of this unit.

The Archimedes Wave Swing performs best for larger and higher waves as shown by its power matrix (Fig. 6).

### 2.2. Waves statistical analysis

The study area’s historical wave conditions were obtained from the ECWMF ERA5 website [18]. The ERA5 data has a spatial resolution of 0.25° in both latitude and longitude. Wave height (Hs), mean period (Tm), and incident wave direction (θ) data from 1979 to 2020 were downloaded.

For the wave climate analysis, we selected Points A1, A2, and A3 (Fig. 2) as points of interest due to their location. The coordinates of these points are given in Table 3.

The statistical analysis revealed that all three points had similar wave characteristics. Therefore, point A1 was selected as the source of information due to its location in front of the port of Ensenada and its unobstructed area, which allows the swell to maintain its intensity as it propagates towards the coast. Based on this information, there are areas with high energy potential, where deploying WECs would be beneficial. Historically, waves at Todos Santos Bay have predominantly arrived from the SW direction (Fig. 7). The most commonly occurring waves have a significant height of 1.25 m, a mean period of 9.5 s, and a peak period of 13.5 s (Figs. 8 and 9).

### 2.3. Wave propagation

WAPO (Wave Propagation On the Coast) was used to propagate wave conditions from the selected point to the coast. The programme solves 2D regular wave propagation by solving the modified mild slope equation, taking into account wave processes such as reflection, refraction,

Table 2  
Main characteristics of the AWS [16].

ITEM	LARGE [M]	DIAMETER [M]	HEIGHT [M]	WIDE [M]	WEIGHT [TON]
FLOATER		9.5	21		206
PONTOON	48		5.5	28	1200
CENTRAL			33.5		120
STRUCTURE					

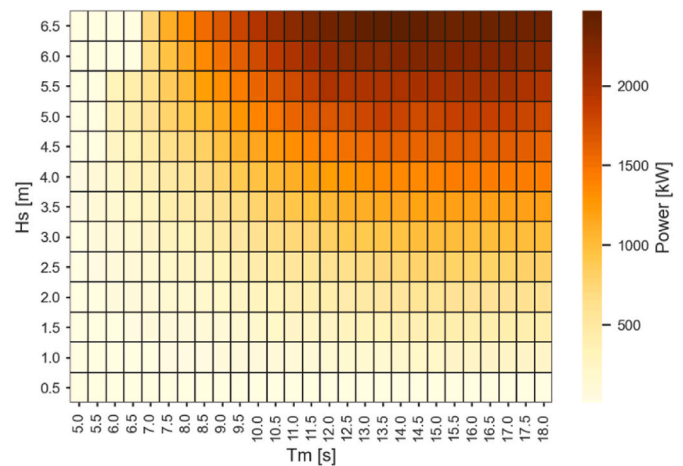


Fig. 6. Archimedes Wave Swing performance matrix [17].

Table 3  
Coordinates of points analysed.

POINT	LOCATION (LAT, LONG) [DEGREES]
A1	31.84, -116.84
A2	31.79, -116.83
A3	31.74, -116.80

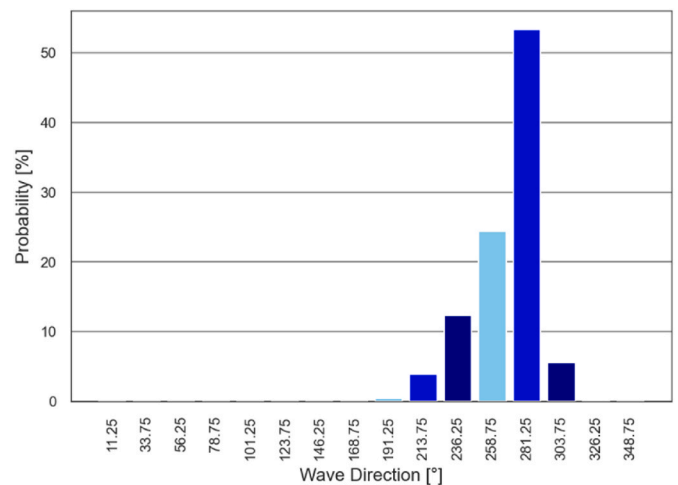


Fig. 7. Historical wave direction (from the North) at point A1 (1979–2020).

diffraction, shoaling and breaking, using a bathymetric grid as input [19]. Further information on the operation and use of the software can be found in Ref. [20].

The Todos Santos Bay area was divided into four quadrants with the aim of propagating the wave in the two deep water quadrants initially, and then starting a new propagation in the shallow water quadrants using the results of the last cells towards the coast. Fig. 10 shows the bathymetric grid used for our modelling, with UTM coordinates Zone 11 N minimum (512640 m E, 3507611 m N) and maximum (537540 m E, 3529706 m N).

From the ER% wave data, conditions with a probability of occurrence of less than 8 % were discarded, and only those shown in Table 4 were used for the modelling.

To illustrate the results obtained from the model, Fig. 11 shows the wave propagation along the study area for wave conditions Hs = 1.25 m, Tm = 10.5 s and θ = 258.75°.

Fig. 11 shows the highest available wave energy in the numerical

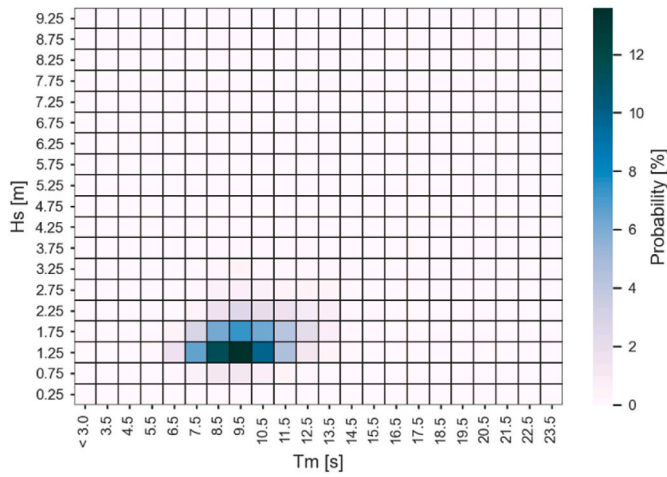


Fig. 8. Joint probability of  $H_s$  and  $T_m$  at point A1 (1979–2020).

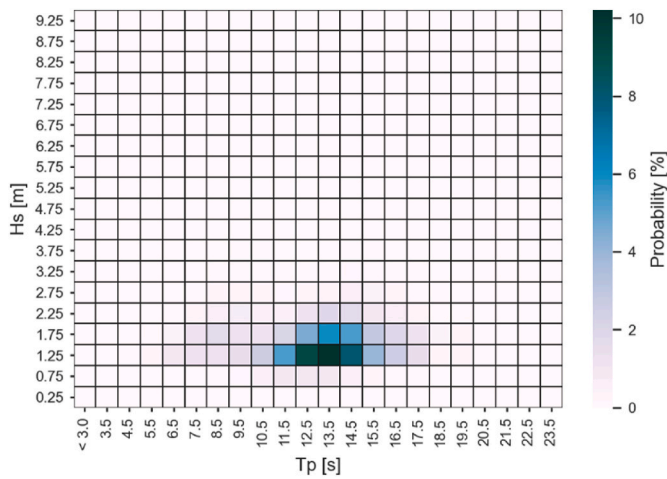


Fig. 9. Joint probability of  $H_s$  and  $T_p$  at point A1 (1979–2020).

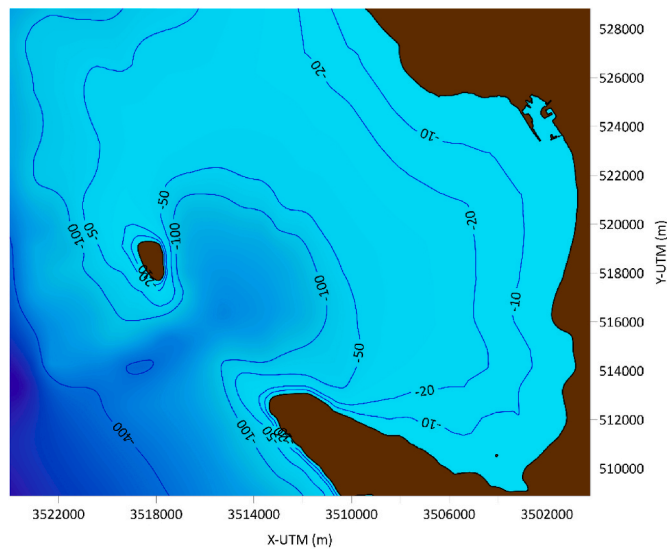


Fig. 10. Bathymetry of todos santos bay.

Table 4  
Data used for WAPO modelling.

$H_s$ [m]	1.25	1.75	2.25					
$T_m$ [s]	8.5	9.5	10.5	11.5	12.5	13.5	14.5	15.5
$\theta$ [°]	236.25		258.75		281.25			

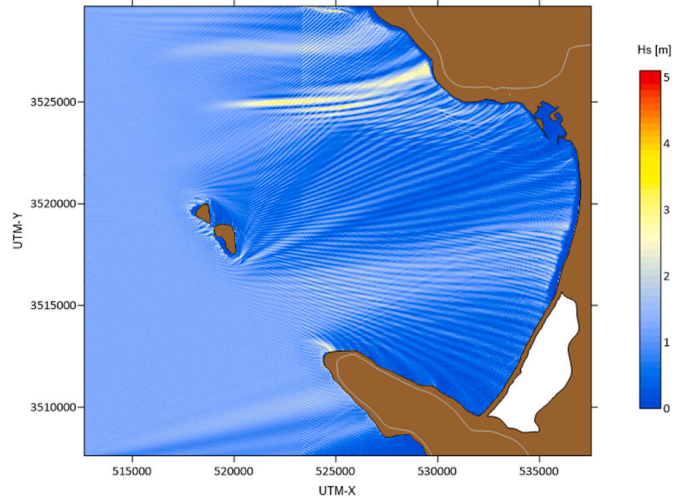


Fig. 11. Wave propagation example with WAPO ( $H_s = 1.25$  m,  $T_m = 10.5$  s and  $\theta = 258.75^\circ$ ).

domain as represented by the yellow area. Therefore, the northern part of the bay is suitable for deployment of a WEC farm.

#### 2.4. Identification of the area with the highest available power

The optimal location for the installation of a WEC farm was determined through a visual inspection of the numerical results. Fig. 12 displays the region with the highest energy potential, shown in blue, for the majority of simulated situations. This area covers a total of 43.25 km<sup>2</sup>.

A grid of 43 x 8 rectangles, each 225 x 555 m long, was constructed within the designated WEC area (Fig. 12). The purpose of this grid was to calculate the theoretical wave potential in specific areas, rather than averaging the power over the entire region.

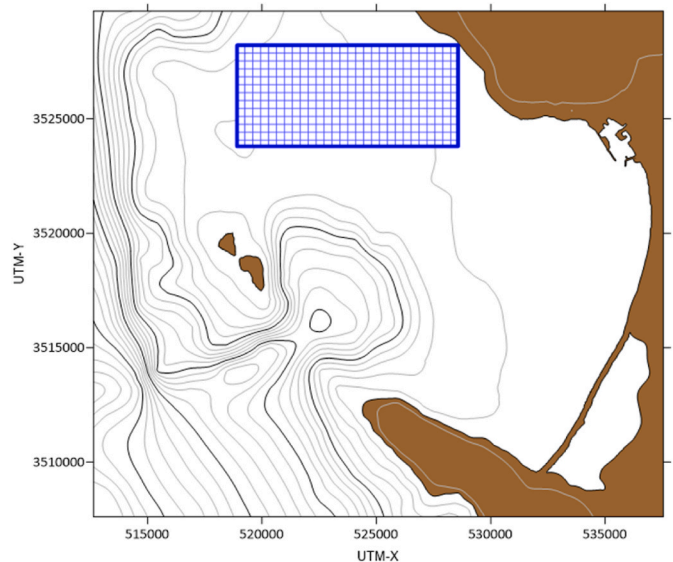


Fig. 12. Area selected for the WEC farm deployment.

## 2.5. WEC farm polygons placement

Seven sub-polygons were created in areas with the highest available energy. The methodology for their selection involved constructing 3 x 3 rectangles and selecting combinations with an average power greater than 20 kW/m.

These seven areas are potential sites for WEC farm installation. Each area has a proposed surface area of 1.12 km<sup>2</sup>, with a length of 675 m to the east and 1665 m to the north. Fig. 13 displays the seven proposed sub-polygons.

## 2.6. WEC array distribution within polygons

### 2.6.1. Transmission coefficient

The transmission coefficient,  $KT$ , for each line of wave energy converters (WECs) in the farm was calculated according to the method described in Ref. [21].

$$P_N = \frac{N_{DN} \cdot K_{TD} \cdot L_y + N_{GN} \cdot D_y \cdot L_y}{L_{tot}} \quad (1)$$

where.

- $P_N$  line number
- $K_{TD}$  transmission coefficient of a single device
- $N_{DN}$  number of devices in line N
- $N_{GN}$  number of gaps in line N
- $L_y$  length of the device perpendicular to wave fronts
- $D_y$  distance between devices
- $L_{tot}$  total length of the farm

From equation (1),  $KT$  from the farm's first line yields

$$K_{T1} = P_1 \quad (2)$$

In turn,  $KT$  from the second line is

$$K_{T2} = K_{T1} \cdot P_2 \quad (3)$$

for the subsequent lines, the following expression is used

$$K_{TN} = \left( \frac{K_{T2}}{K_{T1}} \right)^a \cdot K_{T1}^b, \text{ for } b \geq a \text{ and } N \geq 3 \quad (4)$$

where.

- $a, b$  positive integer numbers

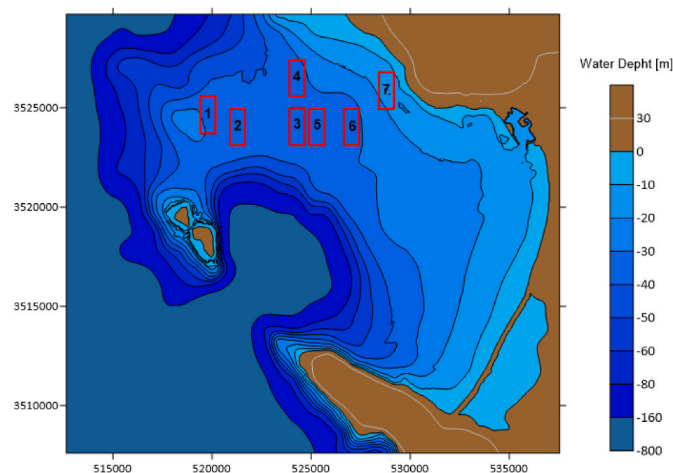


Fig. 13. Areas suitable for WEC farm deployment.

### 2.6.2. Wave Dragon

For the calculation of the transmission coefficient per device,  $K_{TD}$ , the equation by Ref. [22] will be used, that is

$$K_{TD} = -0.087 \frac{L_x}{L_p} + 0.82 \text{ for } 0.905 < \frac{L_x}{L_p} < 1.232 \quad (5)$$

where

- $K_{TD}$  transmission coefficient for a single device
- $L_x$  device length parallel to the wave fronts
- $L_p$  Deep water wave length

The ratio  $L_x/L_p$  was made unitary in this case, obtaining a  $K_{TD} = 0.733$ .

A series of Wave Dragon farms were studied, the array that gave the highest power is described in Table 5 and Fig. 14.

The blue area represents the unit's space, while the white area represents the space between units. For the X direction, it has been assumed that the spacing between devices within the blue box is uniform across all rows. This has little effect on energy production, as a larger area does not add power, it just averages the energy over more data.

**2.6.2.1. Archimedes Wave Swing.** In this case, since there is no equation available for  $K_{TD}$ , we used the average value suggested by Ref. [23] for point absorbers, i.e.,  $K_{TD} = 0.50$ . Table 6 shows the number of devices and farm dimensions is shown in Table 6 and Fig. 15.

## 2.7. Estimation of theoretical and yearly power

The theoretical wave potential was calculated using equation (6) from Ref. [24].

$$P_w = \frac{\rho g^2}{64\pi} H_s^2 T_m \quad (6)$$

where.

- $P_w$  theoretical wave power
- $\rho$  water density
- $g$  acceleration due to earth's gravity
- $H_s$  significant wave height
- $T_m$  mean wave period

Fig. 16 shows the power matrix obtained using equation (6) with the wave conditions present in the polygon under study.

As expected, the theoretical available power (Fig. 16) directly correlates with the significant wave height and the mean period.

The calculation of the yearly power is obtained using equation (7) after determining the total theoretical energy in each rectangle of the deployment area.

$$E = \frac{1}{1000} \sum_{i=1}^{n_T} \sum_{j=1}^{n_H} P_{ij} Q_{ij} t \quad (7)$$

where.

- $E$  yearly theoretical wave energy
- $n_T$  number of wave period classes
- $n_H$  number of wave height classes
- $P_{ij}$  sea state probability of occurrence
- $Q_{ij}$  theoretical power matrix

The yearly theoretical energy that can be produced in each rectangle of the polygon is shown in Fig. 17.

The distribution of wave power within the deployment area is determined by the combination of propagated wave conditions.

**Table 5**  
Wave Dragon farm description.

DEVICES	LINES	DEVICES IN ODD LINES	DEVICES IN EVEN LINES	FARM X LENGTH [M]	FARM Y LENGTH [M]	MARINE AREA USED [KM <sup>2</sup> ]
5	2	3	2	540	1350	0.73

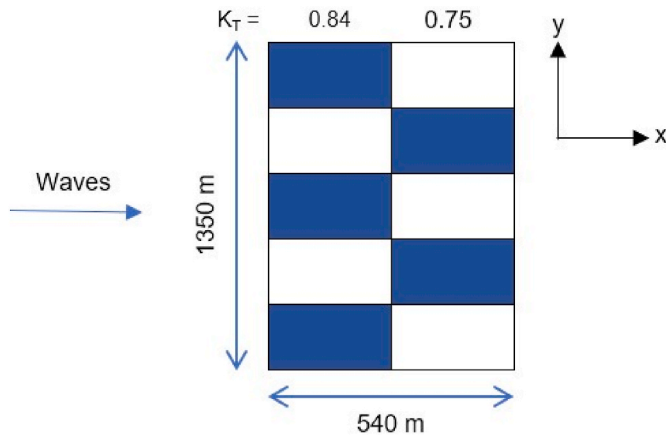


Fig. 14. Wave Dragon farm array and transmission coefficient by line.

According to Fig. 17, the most suitable location for the farm is at coordinates 3525730 N and 527348 W. However, it is important to consider the farm's performance and energy costs before making a final decision.

2.8. Estimation of levelized cost of energy (LCOE)

The Levelized Cost of Energy (LCOE) is the present value of the net cost (\$/kWh) of producing energy from a power plant over its lifespan. LCOE includes all costs associated with investment, fuel, operation and maintenance. Equation (8) illustrates the mathematical expression of this concept.

$$VPC = \sum \frac{LCOE \cdot Q_t}{(1+i)^t} \tag{8}$$

where.

- VPC present value of the electric plant costs
- Q<sub>t</sub> net electric generation along the period t
- LCOE levelized cost of energy

From equation (8), LCOE is

$$LCOE = \frac{VPC}{\sum \frac{Q_t}{(1+i)^t}} = \frac{VPC}{VPQ} \tag{9}$$

where.

VPQ present value of electric generation.

The levelized capacity charge (LCC) is the amount of money a power plant must receive, expressed in \$/MW/year, to recoup its investment. The LCC generally covers the debt incurred and interest earned, equity contribution and after-tax returns, and income taxes.

The main benefit of this measure is that it explicitly stated the financing framework (debt-to-equity) and the amount of income taxes,

**Table 6**  
Number of AWS devices on farm.

DEVICES	LINES	DEVICES IN ODD LINES	DEVICES IN EVEN LINES	FARM X LENGTH [M]	FARM Y LENGTH [M]	MARINE AREA USED [KM <sup>2</sup> ]
54	4	14	13	480	1620	0.78

providing an annual summary of the cost of each item. The LCC is used in various ways in to calculate the Levelized Cost of Energy (LCOE). As it is expressed in terms of power, it can be converted into its \$/MWh equivalent for a given plant factor, as shown in equation (10).

$$LCOE = \frac{LCC}{t \cdot CF} \tag{10}$$

where.

- LCC levelized capacity charge
- t yearly hours
- CF plant capacity factor

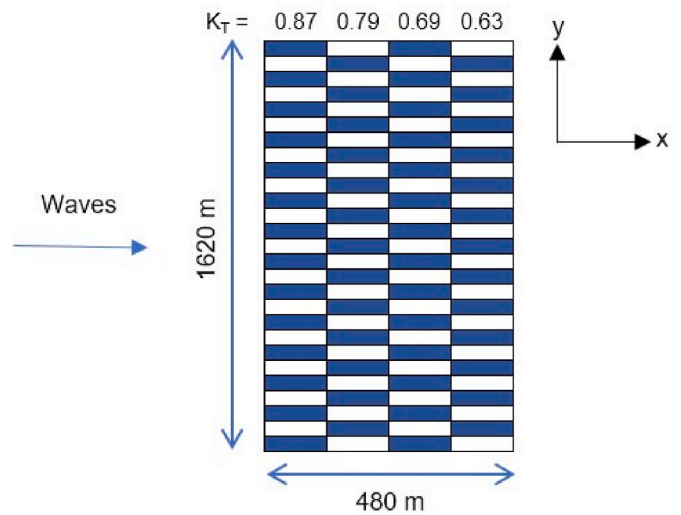


Fig. 15. Archimedes Wave Swing array and transmission coefficient by line.

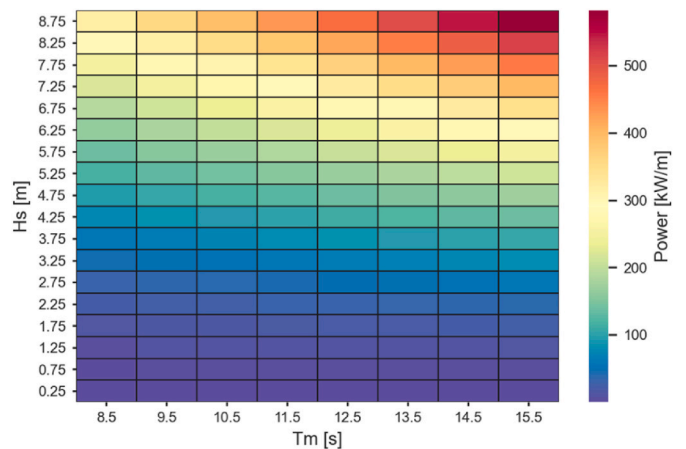


Fig. 16. Theoretical wave power matrix within the WEC deployment area.

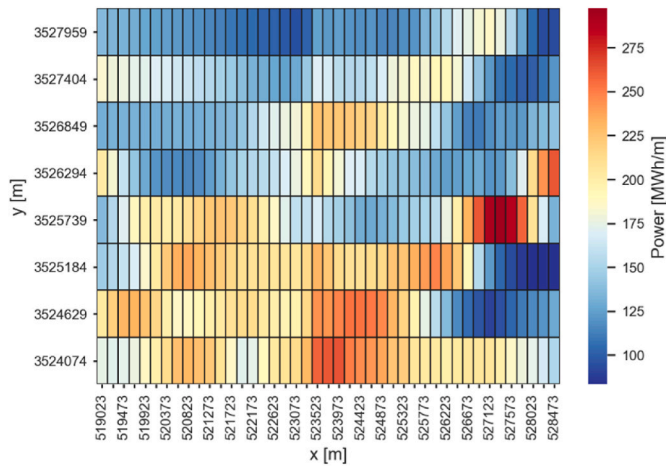


Fig. 17. Yearly theoretical energy within the deployment area.

### 3. Results

#### 3.1. Wave Dragon farm

Fig. 18 shows the annual electrical energy produced by a Wave Dragon device under the wave conditions of the study polygon without *KT* estimation. The farm proposal that generates more electricity is labelled E.

It is evident that farm 7 (Fig. 18) corresponds to the area of higher theoretical power. However, when considering the farm performance, the optimal location is situated to the west.

Fig. 19 shows the yearly electrical energy produced by each possible farm in the study area, considering a staggered arrangement and calculating *KT* for each line. To determine the optimal farm, we analysed 408 possible farm combinations.

#### 3.2. Archimedes wave swing farm

Fig. 20 shows the yearly electric power produced by Archimedes Wave Swing farms without computing *KT*.

Fig. 20 demonstrates that the optimal location for the farm, as determined by theoretical computation, may not be the most suitable when considering farm performance, including WEC power matrix and wave damping across WEC lines.

Fig. 21 shows the yearly electricity generated by each possible farm in the study area, considering a staggered arrangement and the *KT* per line. A total of 3696 farms were analysed.

#### 3.3. Capacity factor

The capacity factor, *CF*, is the ratio of electrical energy produced by a device to the maximum amount of electrical power it could generate under optimal conditions. *CF* is usually calculated annually using equation (11).

$$CF = \frac{E_{prod}}{E_{max}} \quad (11)$$

where,

- CF* capacity factor
- $E_{prod}$  annual power produced
- $E_{max}$  maximum power produced in a year

The study site's *CF* was calculated based on the electric power generated per farm, as illustrated in Figs. 18 and 20, with  $E_{max}$  representing the maximum value. This value was obtained from the

prevailing wave conditions and represents the maximum energy that a WEC farm could generate if deployed at the proposed site. To calculate  $E_{prod}$ , a series of thresholds were considered for each technology to determine the amount of energy constantly produced per farm.

##### 3.3.1. Capacity factor for Wave Dragon farms

To calculate  $E_{prod}$ , nine energy thresholds were used, ranging from 200 kW to 5000 kW, with a uniform increase of 800 kW (Table 7). The power matrix shown in Fig. 4 was used to define these thresholds, ensuring coverage of all values of the power matrix.

##### 3.3.2. Capacity factor for Archimedes Wave Swing farms

Nine thresholds were used to calculate  $E_{prod}$  based on the theoretical power matrix shown in Fig. 6, similar to the case of Wave Dragon devices. The thresholds for Archimedes Wave Swing range from 30 kW to 2190 kW with a uniform increment of 270 kW (Table 8).

#### 3.4. Levelized capacity cost calculation

To calculate the CCN (capacity cost), it is assumed that the wave power plant has a useful life of 30 years (period 2025–2054) without considering the salvage value. We also assume that the plant is financed with 65 % debt, which is contracted in dollars for a term of 15 years with an interest rate of 4.51 % p. a. (already including the interest tax for credit with a foreign bank), while own resources cover the remaining 35 % with a yield of 12.4 % after tax.

During the 30-month construction period starting in 2022, investment disbursements will be made in equal monthly instalments. The disbursements will follow the financing structure, with 65 % being debt and 35 % equity. The interest generated during construction will be used as the basis for the financial payments (amortisation and interest) during the operation of the wave power plant.

However, it is crucial to note that the equity disbursed during the construction period remains idle, resulting in an "opportunity cost". This refers to the earnings that were not generated during construction, which will be factored in when updating the value of the equity at the beginning of the operation. To calculate the annual rate at which the investment will increase, the WACC (weighted average capital cost) was utilised, as per equation (12).

$$WACC = T_{int}F_d + R_I F_p \quad (12)$$

where,

- $T_{int}$  interest rate at which the debt was contracted
- $F_d$  debt financing
- $F_p$  equity financing
- $R_I$  rate of return

However, when making monthly disbursements, it is necessary to calculate the monthly rate based on the annual rate using equation (13). The monthly rate is defined as the rate that cumulatively reproduces the yearly rate over twelve months.

Thus, during construction, the weighted average cost of the two sources of financing will be 7.27 %. Therefore, using equation (13), the total investment at the start of the operation will increase by a total of 9 %, comprising a 5.5 % increase in debt at the beginning of the operation and a 15.6 % increase in equity.

$$(1 + T_{men})^{12} = (1 + T_{an}) \rightarrow T_{men} = (1 + T_{an})^{1/12} - 1 \quad (13)$$

where,

- $T_{men}$  monthly rate
- $T_{an}$  annual rate

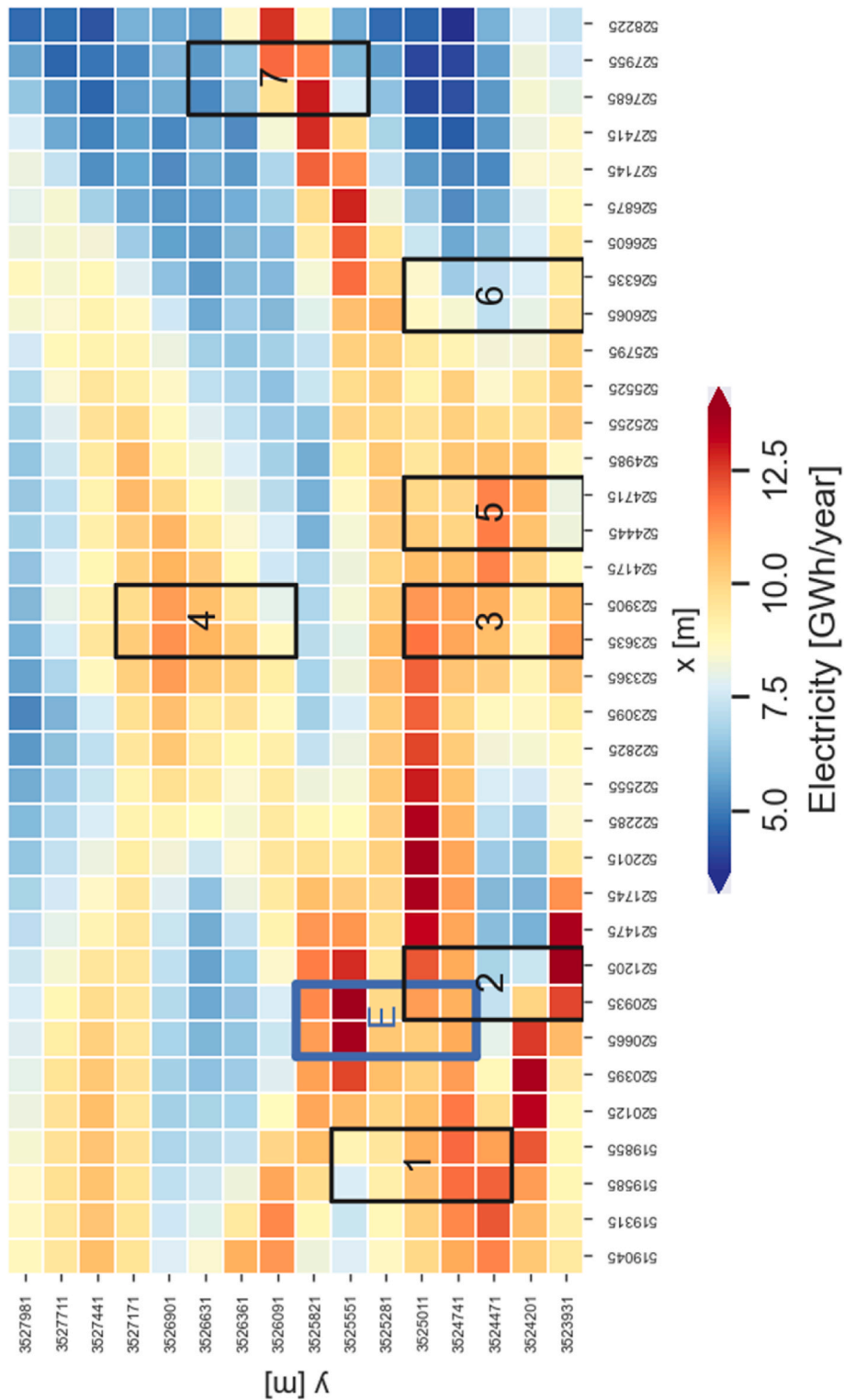


Fig. 18. Theoretical maximum electric power generated by the Wave Dragon farms; E shows the best option.

### 3.4.1. Technical parameters

The nominal power of each Wave Dragon and Archimedes Wave Swing farm is 20 MW and 108 MW, respectively. At the output of the generating plant, 2.5 % of the energy generated will be consumed by the plant itself.

When calculating the CCN, it is important to specify the net power available under the conditions in which the plant is installed. Based on the above, the power for each farm ranges between 14 % and 26 % of its

maximum capacity. During the first year of operation, the net capacity at the installation site is reduced. Additionally, a yearly average deterioration rate of 0.20 % is considered. Technical parameters for Wave Dragon farms are presented in Table 9, while those for Archimedes Wave Swing farms are shown in Table 10.

### 3.4.2. Inflation and taxes

The average annual inflation rates for Mexico and the United States

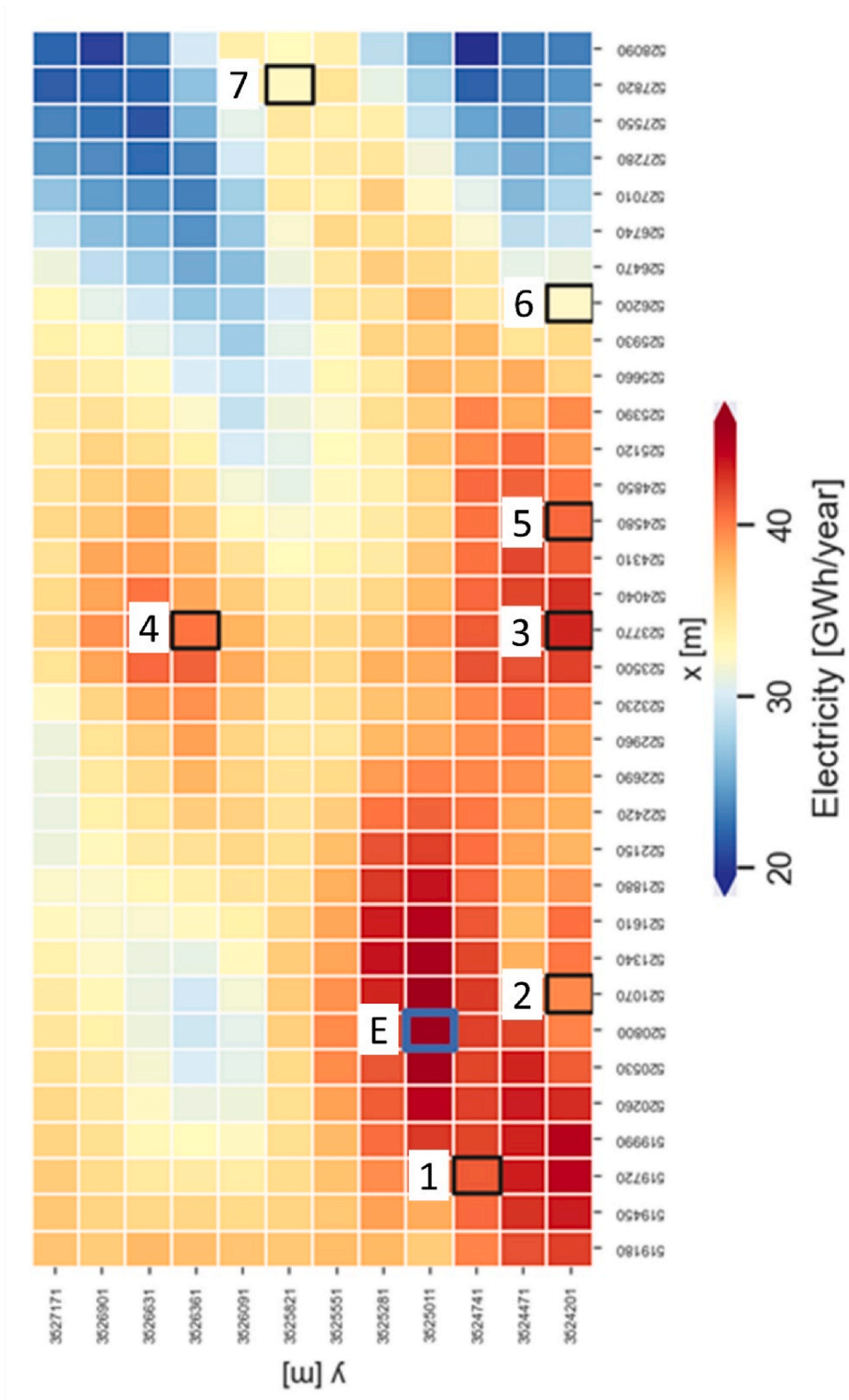


Fig. 19. Electric energy generated by Wave Dragon farms; the one generating the device producing the highest power is shown in a blue rectangle.

over the last decade were 3.5 % and 2.0 %, respectively. In addition, being financed by a foreign bank, an interest tax of 4.9 % must be paid when financed by a foreign bank, as per Articles 166-I and II of the income tax law. Table 11 provides a summary of the inflation and depreciation rates in the renewable energy sector in Mexico.

### 3.4.3. Rate of return

The capital model assessment (CAPM) was used to calculate the rate

of return. This model, commonly used to evaluate investment projects in both developed and emerging countries, and it calculates the rate of return generated on invested equity capital. Equation (14) displays the parameters involved in the calculation.

$$R_I = R_F + \beta_i(R_M - R_F) + R_P \tag{14}$$

where.

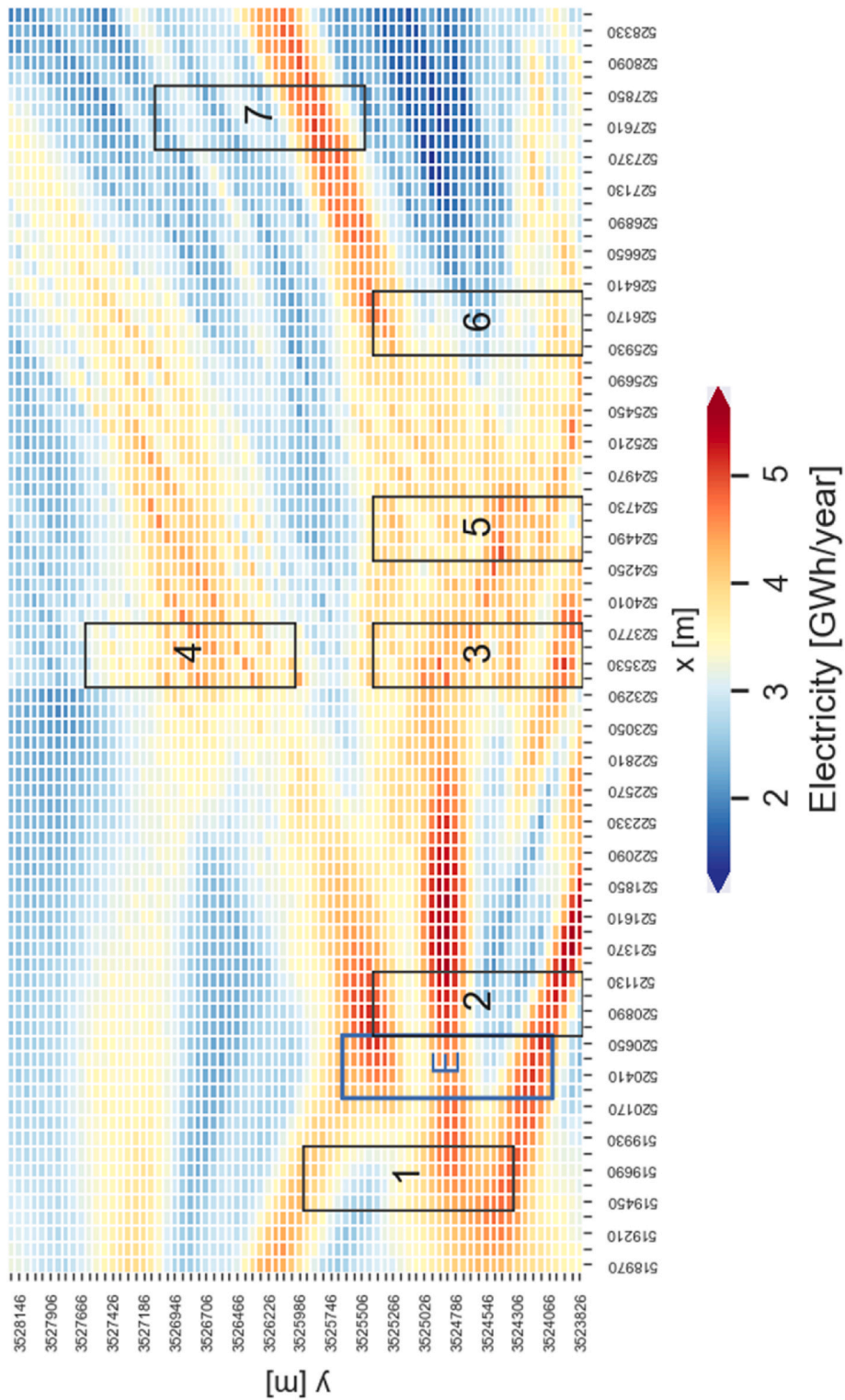


Fig. 20. Theoretical maximum electric power generated by the Wave Dragon farms; E shows the best option.

- $R_I$  return rate
- $R_F$  risk-free rate
- $R_M$  stock market rate of return
- $\beta_i$  company specific risk indicator
- $R_P$  country risk bonus

Table 12 shows the rate of return obtained from Equation (14).

#### 3.4.4. Cost per device

The cost per device was calculated based on its weight, specifically the steel/ballast ratio for each technology was considered and multiplied by the average cost of the material used. Table 13 shows the steel and ballast proportions for the devices being studied.

The steel/ballast ratio for the Wave Dragon was obtained from the reported weights of a model tested off the coast of Portugal [30]. However, the Archimedes Wave Swing is considered an all-steel device

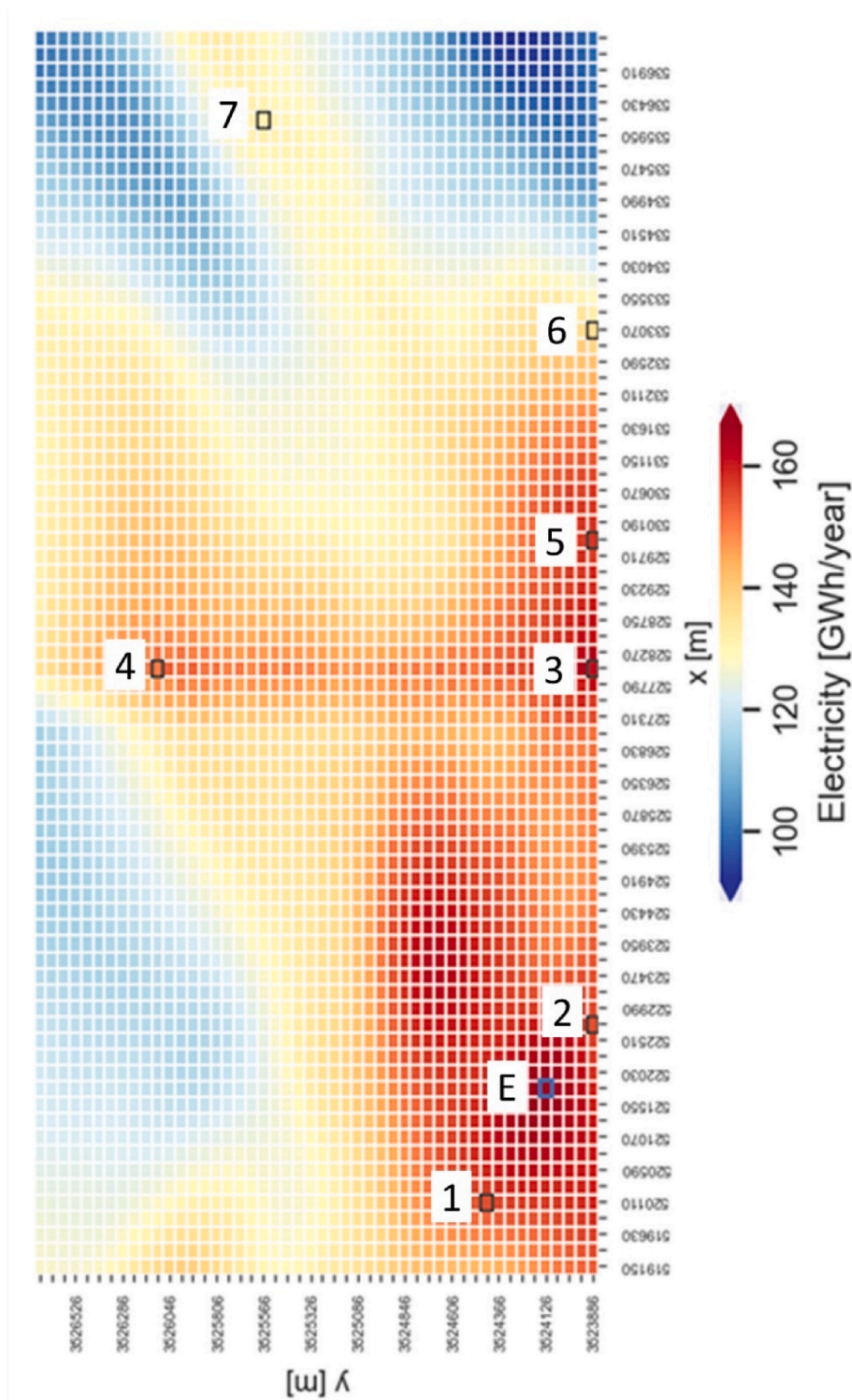


Fig. 21. Electric energy generated by Archimedes Wave Swing farms; the one generating the device producing the highest power is shown in a blue rectangle.

as it is submerged and does not require a ballast.

The average steel price from 2000 to 2021 is 4450 CNY/ton, equivalent to 700 USD/ton [31].

In contrast, ballast is assigned a price of 100 USD/ton, as inexpensive materials such as water are commonly used. Table 14 displays the cost per device and farm based on the established prices and their steel/ballast ratio.

### 3.4.5. Cost per infrastructure

The infrastructure cost for a WEC device farm was calculated using the methodology described in Ref. [32]. This methodology assigns a percentage of the cost to the different items that make up the infrastructure.

In this work, the cost of the devices that make up the farm was used as the basis. Table 15 shows the costs for each type of infrastructure, adapted as a percentage of these costs.

In a similar way to the cost obtained by infrastructure type in the

**Table 7**  
Capacity factor and generation time for Wave Dragon farms.

FARM	$E_{MAX}$ [GWH/Y]	$E_{PROD}$ [GWH/Y]	CF [%]	TIME GENERATING [%]
1	41.39	29.67	72 %	81 %
2	39.68	29.02	73 %	71 %
3	43.27	34.01	79 %	63 %
4	40.42	30.63	76 %	67 %
5	40.87	31.88	78 %	62 %
6	32.22	24.44	76 %	53 %
7	32.48	24.59	76 %	54 %
E	45.88	34.73	76 %	75 %

**Table 8**  
Capacity factor and generation time Archimedes Wave Swing farms.

FARM	$E_{MAX}$ [GWH/Y]	$E_{PROD}$ [GWH/Y]	CF [%]	TIME GENERATING [%]
1	155.00	93.49	60 %	99 %
2	155.13	96.94	62 %	98 %
3	161.05	109.70	68 %	93 %
4	150.35	96.14	64 %	94 %
5	157.80	106.72	68 %	92 %
6	136.30	88.69	65 %	88 %
7	131.41	82.99	63 %	91 %
E	166.53	106.25	64 %	99 %

**Table 9**  
Maximum power generated per Wave Dragon farm.

FARM	SINGLE DEVICE POWER [MW]	DEVICES	FARM POWER [MW]	MAX AVAILABLE POWER [MW]	POWER CONVERTED [%]
1	4	5	20	4.73	24
2				4.53	23
3				4.94	25
4				4.61	23
5				4.67	23
6				3.68	18
7				3.71	19
E				5.24	26

**Table 10**  
Maximum power generated per Archimedes Wave Swing farm.

FARM	SINGLE DEVICE POWER [MW]	DEVICES	FARM POWER [MW]	MAX POWER AVAILABLE [MW]	POWER CONVERTED [%]
1	2	54	108	17.69	16
2				17.71	16
3				18.38	17
4				17.16	16
5				18.01	17
6				15.56	14
7				15.00	14
E				19.01	18

**Table 11**  
Taxes and Inflation used [25,26].

VALUE	ANNUAL RATE [%]
INCOME TAX RATE	30.0
MACHINERY AND EQUIPMENT	100.0 (FIRST YEAR)
CIVIL WORKS	5.0
PRE-OPERATING EXPENSES	10.0
INTEREST TAX RATE	4.9
INFLATION RATE FOR DOLLARS (US)	2.0
INFLATION RATE FOR PESOS (MXN)	3.5

**Table 12**  
Calculated rate of return [27–29].

RISK FREE RATE, $R_F$	COUNTRY RISK BONUS, $R_P$	BUSINESS LINE RISK, $B_1$	EQUITY MARKET YIELD, $R_M$	RATE OF RETURN, $R_1$
3.77 %	2.64 %	1.05 %	9.01 %	12.40 %

**Table 13**  
Steel and ballast proportions for each device.

DEVICE	STEEL [%]	BALLAST [%]
WAVE DRAGON	63	37
ARCHIMEDES WAVE SWING	100	0

**Table 14**  
Prices per device and per farm.

VALUE	WAVE DRAGON	ARCHIMEDES WAVE SWING
DEVICE WEIGHT [TON]	22,000	1526
STEEL WEIGHT [TON]	13,860	1526
BALLAS WEIGHT [TON]	8140	0
COST PER DEVICE [USD X1000]	10,516	1068
DEVICES	5	54
COST PER FARM [USD X1000]	52,580	57682

**Table 15**  
Infrastructure cost as a percentage of device.

TYPE OF INFRASTRUCTURE	COST OF WAVE DRAGON DEVICES ON FARM [%]	COST OF ARCHIMEDES WAVE SWING ON FARM [%]
PLANNING AND INSTALLATION	10	10
MOORING	10	2
WIRING	5	5
ELECTRICAL INTERCONNECTION NETWORK	1	1
DECOMMISSIONING	10	10
OTHERS	5	5
MANAGEMENT COSTS	5	5
PERMITS	2	2
ENVIRONMENTAL STUDIES	0.05	0.05
REPLACEMENT COSTS	90	90
REPLACEMENT PARTS	2	2

previous table, a factor was applied to simulate cost-sharing among a set of devices resulting in a reduced total cost of the work. Table 16 shows the cost per infrastructure that each farm will incur when applying a sharing factor of  $0.85 F_{comp}$ .

3.4.6. Levelized capacity charge results

Using the aforementioned parameters, the CCN was calculated for each technology, as shown in Table 17 for Wave Dragon farms; and Table 18 for Archimedes Wave Swing farms.

3.5. Levelized cost of energy Wave Dragon farm

Table 19 shows the LCOE for each proposed farm, as derived from the results obtained by CCN.

Table 19 highlights that farms E and 3 have the lowest cost. However, Table 7 shows that farm E has the highest constancy of electricity generation.

Fig. 22 displays the cash flow that farm E will have during its lifetime. It is clear that once the debt is covered, the net income grows at a

**Table 16**

Total infrastructure cost.

INFRASTRUCTURE TYPE	INFRASTRUCTURE COST WAVE DRAGON FARM [USD X1000]	INFRASTRUCTURE COST ARCHIMEDES WAVE SWING FARM [USD X1000]
PLANNING AND INSTALLATION	4469.3	4903.0
MOORING	4469.3	980.6
WIRING	2234.7	2451.5
ELECTRICAL INTERCONNECTION NETWORK	446.9	490.3
DECOMMISSIONING	4469.3	4903.0
OTHERS	2234.7	2451.5
MANAGEMENT COSTS	2234.7	2451.5
PERMITS	893.9	980.6
ENVIRONMENTAL STUDIES	22.3	24.5
REPLACEMENT COSTS	40,223.7	44,127.3
REPLACEMENT PARTS	893.9	980.6

**Table 17**

Levelized capacity charge for Wave Dragon farms.

Farm	Levelized capacity charge 2022 [\$ <sub>2022</sub> /MWy]	Levelized capacity charge present [\$/MWy]
1	2,187,571	2,646,397
2	2,282,209	2,760,884
3	2,092,727	2,531,660
4	2,240,128	2,709,976
5	2,215,653	2,680,368
6	2,810,391	3,399,848
7	2,387,574	3,372,382
E	1,973,623	2,387,574

**Table 18**

Levelized capacity charge for Archimedes Wave Swing farms.

Farm	Levelized capacity charge 2022 [\$ <sub>2022</sub> /MWy]	Levelized capacity charge present [\$/MWy]
1	620,097	750,213
2	619,606	749,618
3	596,818	722,049
4	639,292	773,435
5	609,110	736,920
6	705,212	853,188
7	731,450	884,931
E	577,164	698,271

**Table 19**

LCOE for farm with WD devices.

Farm	LCOE			
	2002		Present	
	\$ <sub>2022</sub> /MWh	\$ <sub>2022</sub> /kWh	\$/MWh	\$/kWh
1	350.4	0.35	423.9	0.42
2	356.2	0.36	430.9	0.43
3	303.9	0.30	367.7	0.37
4	337.4	0.34	408.2	0.41
5	324.3	0.32	392.3	0.39
6	422.9	0.42	511.6	0.51
7	360.0	0.36	508.5	0.51
E	<b>297.6</b>	<b>0.30</b>	<b>360.0</b>	<b>0.36</b>

similar rate to previous years.

Fig. 23 shows the debt coverage ratio (DCR) [33]. The plant will generate enough net income to cover the debt plus 40 % of it, indicating a high probability of borrowing by the financial institution.

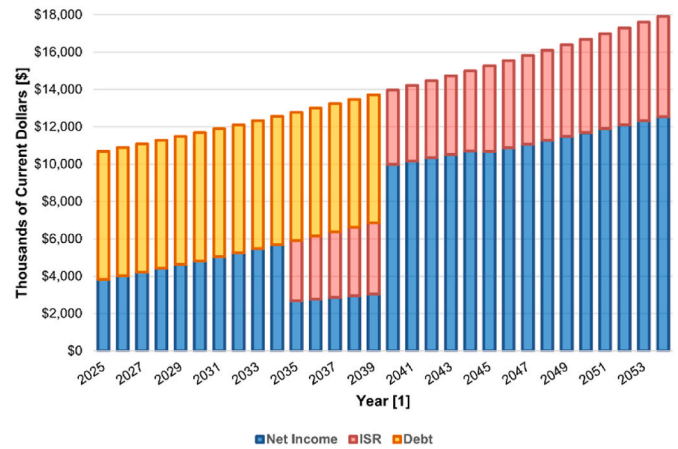


**Fig. 22.** Cash Flow for Farm E with Wave Dragon devices.

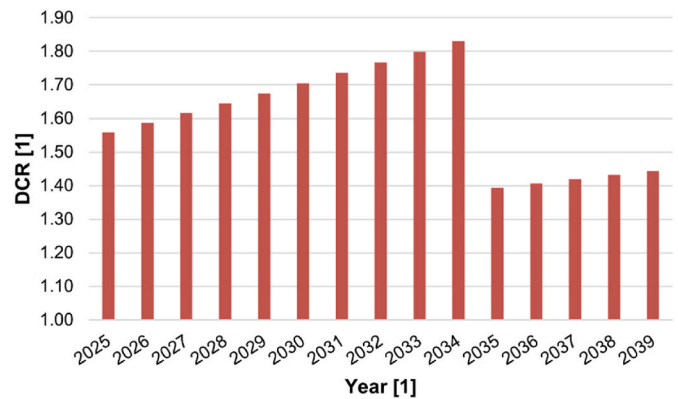


**Fig. 23.** Debt Coverage Ratio for Wave Dragon farm.

### 3.6. Levelized cost of energy archimedes wave swing farm

Table 20 displays the LCOE for each proposed farm of Archimedes Wave Swing devices, similar to the Wave Dragon case.

Table 20 highlights that farms E, 3 and 5 have the lowest cost. However, Table 8 shows that farm E has the highest constancy of electricity generation, making it the best option.

Fig. 24 shows the cash flow that farm E will have during its lifetime.

The financing structure is the same for both technologies, resulting in similar percentages for net profit, taxes, and debt. Nevertheless, the cash flow is higher in this case, leading to a higher net profit.

Finally, Fig. 25 displays the DCR, which is very similar to Fig. 23 as they share the same financing structure.

**Table 20**

LCOE for Archimedes Wave Swing farm.

Farm	LCOE			
	2022		Present	
	\$ <sub>2022</sub> /MWh	\$ <sub>2022</sub> /kWh	\$/MWh	\$/kWh
1	117.4	0.12	142.0	0.14
2	113.2	0.11	136.9	0.14
3	100.0	0.10	121.0	0.12
4	114.1	0.11	138.1	0.14
5	102.8	0.10	124.4	0.12
6	123.7	0.12	149.7	0.15
7	132.2	0.13	160.0	0.16
E	103.3	0.10	124.9	0.12

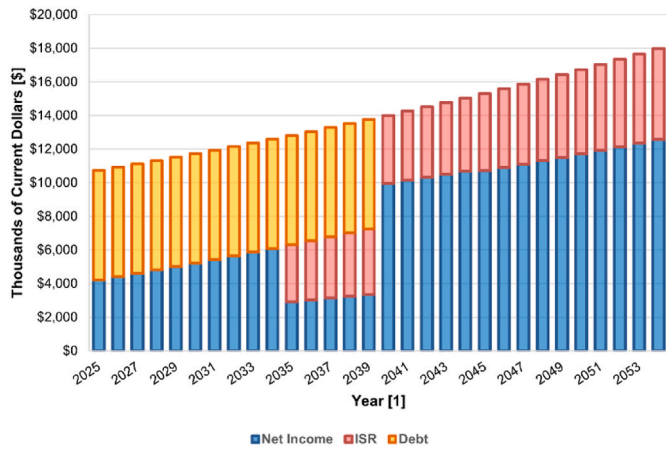


Fig. 24. Cash Flow for Farm E with Archimedes Wave Swing devices.

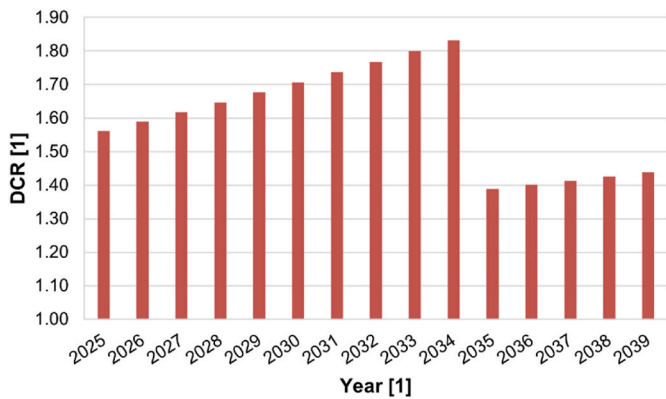


Fig. 25. Debt Coverage Ratio for Archimedes Wave Swing farm.

4. Discussion

The assessment of the feasibility of an entire wave energy converter (WEC) farm, taking into account both the available energy distribution and the overall farm performance, demonstrates that relying solely on theoretical computations may not yield the optimal location for WEC farms.

While determining the location and energy cost based on the availability factor [3] works well for analysing a single device, it may be inaccurate for a farm due to the interaction between wave devices.

The levelized cost of energy (LCOE) may depend on the number of devices considered [5]. According to this research, smaller devices, although more numerous, produce energy at a lower cost. Additionally, designing for low LCOE can be achieved by considering whole farms [7].

4.1. Comparison between technologies

The annual generation time for farms using Archimedes Wave Swing (AWS) devices is significantly longer than that achieved using Wave Dragon (WD). This is mainly due to the fact that the AWS device can operate under most wave conditions at the site, whereas the WD devices operate intermittently by working under wave conditions that occur infrequently at the site.

Fig. 26 compares all the analysed farms, showing that farms 1 and E for both technologies have the longest generation time.

The Archimedes Wave Swing devices generate more annual electrical energy than the Wave Dragon farms. This is mainly due to the higher number of devices installed. Although both technologies used the same area, the ratio of Space Used/Nominal Power per device was much

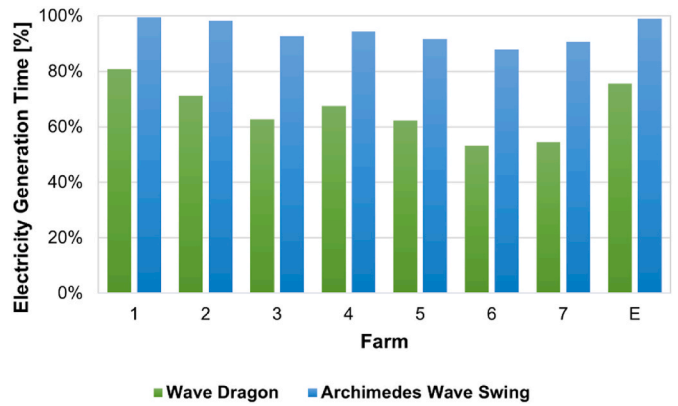


Fig. 26. Generation time comparison between farms and devices.

higher for the AWS farms. To summarise, while Wave Dragon farms may have a higher FC and favourable wave conditions for generating electrical energy, they are outperformed by the number of installed Archimedes Wave Swing devices. Therefore, for the study site farm, Archimedes Wave Swing devices are the better option.

According to Fig. 27, farms 3, 5, and E generate the highest amount of electrical energy for both technologies.

Using the financing structure outlined above, it was determined that farms 3, 5, and E had the lowest cost (\$/kWh) for both technologies.

Fig. 28 displays the LCOE in constant dollars for each analysed farm. The Archimedes Wave Swing farms produce electricity at a significantly lower cost.

However, the US Energy Information Administration [34] presents projected LCOE values for electric power generation plants in Table 21. These values are updated to 2022 dollars, considering an inflation rate of 2.0 %.

It is important to note that the LCOE for different technologies was calculated based on the US economy, whereas this research considers the Mexican economy. Therefore, the cost difference may be even lower than shown if analysed under the same economic conditions.

4.2. Sensitivity analysis

Based on the results from the previous section, the Archimedes Wave Swing farms 3, 5 and E had the lowest LCOE. However, farm E had the longest generation time and was selected for sensitivity analysis. The purpose of this analysis is to identify the impact of a set of variables on the calculation of the LCOE. Table 22 shows the selected variables, with capacity factor being used as a direct indicator of equipment performance. The debt-equity structure indicates the project’s susceptibility to financing and macroeconomic stability. The usage sharing factor

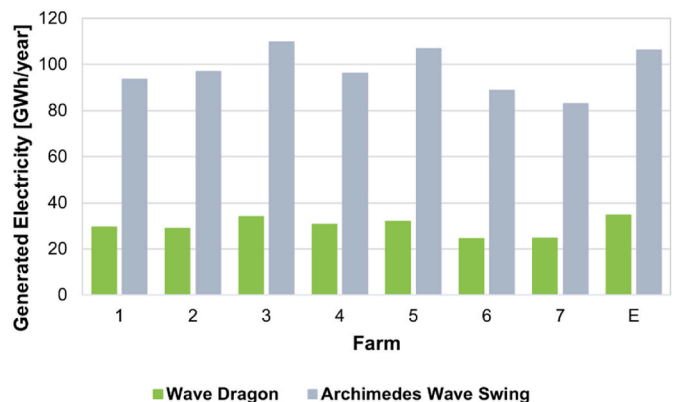


Fig. 27. Comparison of electricity generated between farms and devices.

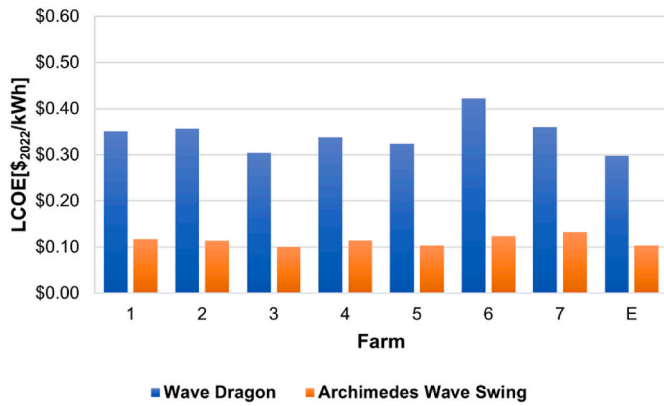


Fig. 28. Comparison of LCOE between farms and devices.

Table 21  
Comparison of LCOE between technologies.

Technology	LCOE [\$2022/kWh]	Change against farm E [%]	
		Wave Dragon	Archimedes Wave Swing
Combined cycle	0.036	-88	-65
Gas turbine	0.112	-62	9
Geothermal	0.036	-88	-66
Offshore wind	0.120	-60	16
Onshore wind	0.033	-89	-68
Photovoltaic	0.030	-90	-71

Table 22  
Variables tested in the sensitivity analysis.

Variable	Base scenario	LCOE Constant [\$2022/kWh]	LCOE Current [\$2022/kWh]
Capacity Factor [%]	64	0.10	0.12
Debt/Equity Structure [%]	65		
Usage Sharing Factor [%]	85		
Steel Price [\$/Ton]	700		
Site Capacity [%]	18		

explains how economies of scale are generated. The steel price is an indicator of construction materials, and the site capacity relates to the suitability of the equipment for the proposed site.

Fig. 29 shows the impact of the capacity factor on the LCOE. A low CF results in a significant increase in \$/kWh, while the impact is greatly reduced when the CF is higher than 70 %. For instance, a CF of 40 % would increase the cost by 59.5 % compared to the base case, whereas a

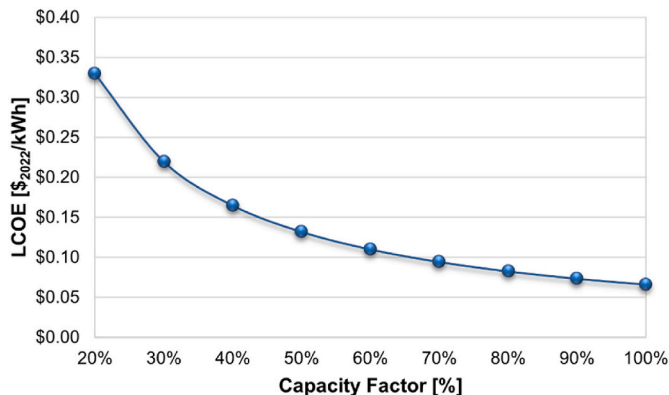


Fig. 29. Impact of capacity factor on LCOE.

CF of 90 % would reduce the cost by 29.1 %.

The percentage of debt acquired to finance the project varies by  $\pm 5.5$  % of the cost for every  $\pm 10$  % of the debt incurred. The variable has the most significant impact on the DCR (Fig. 30). A debt ratio of over 70 % implies that the likelihood of obtaining a loan from a financial institution is minimal and may not even be covered.

The impact of shared use is directly proportional, with a cost variation of  $\pm 5.7$  % for every  $\pm 10$  % of the shared use factor. Fig. 31 illustrates that for a 100 % shared factor, the LCOE would be 12 US cents, while for a 70 % shared factor, the LCOE would be 9 US cents.

The effect of steel prices on the LCOE is also linear, changing at a rate of  $\pm 7.2$  % for every  $\pm \$50$ /tonne. Fig. 32 depicts the relationship between LCOE and steel prices.

The effect of net capacity on the levelized cost of energy (LCOE) can be summarized as follows: if the site conditions are unsuitable for the installed wave energy converters (WECs), the cost per kilowatt-hour (\$/kWh) increases significantly. Conversely, if the site is suitable, the cost of electricity can be reduced. For instance, if the WEC farm converts only 5 % of the available energy, the cost would increase by 252 % compared to the base case. However, if it converts 35 %, the price would decrease by 49.7 % (see Fig. 33).

The research results provide more detailed information than previous efforts e.g. Ref. [8] as it covers from the deep-water waves to the distribution of devices within the farms and its interaction with local waves. The method presented is an improvement from the theoretical power availability and cost calculation shown in Refs. [35,36].

#### 4.3. Additional uses

The primary advantage of installing a WEC farm is coastal protection, in addition to providing electricity and clean energy. While traditional alternatives may offer better protection, a WEC farm provides a sustainable solution by offering two services from a single construction site. However, it is important to evaluate whether the protection provided by these devices is suitable for the beach's intended use.

Farm E is equipped with Archimedes Wave Swing devices and is located 9.0 km from the fishing port of El Sauzal. It has the potential to mitigate beach erosion on the surrounding coasts. However, it is important to assess whether the size of the farm would interfere with shipping lanes or coastal activities in the region.

The State of Baja California operates as an isolated system, producing its own electricity and is not part of the National Interconnected System. Currently, the net energy produced by the WEC farm (1740 MW) covers the demand (1724 MW), with the surplus energy being exported, mainly to the United States [37]. It is important to note that the surplus energy is mainly exported to the United States. In this scenario, it is crucial to produce the lowest possible LCOE to be competitive and, more importantly, to effectively improve the quality of life for coastal communities.

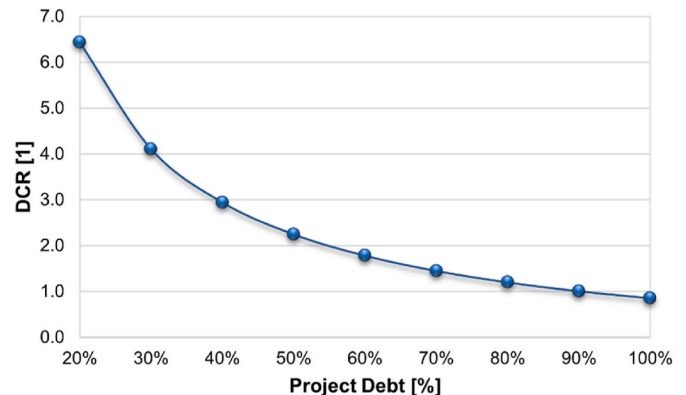


Fig. 30. Impact of the debt ratio on the lending probability.

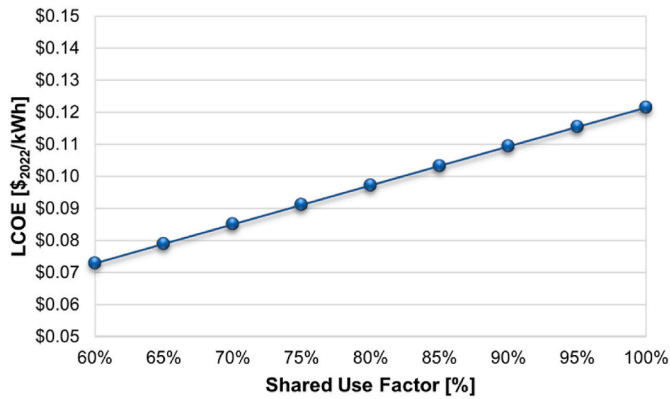


Fig. 31. Impact of the shared use factor on LCOE.

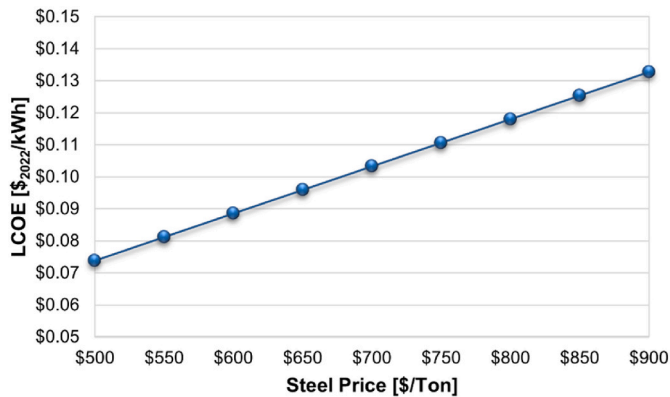


Fig. 32. Impact of steel price on LCOE.

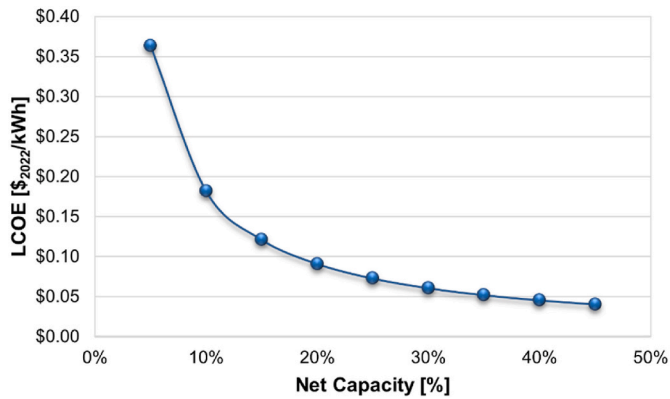


Fig. 33. Impact of capacity utilisation on LCOE.

This may be strongly enhanced with the methodology presented in this study.

Therefore, connecting the WEC farm to the grid would be unattractive. A more feasible option would be to supply the port of El Sauzal with electricity. As a fishing area, it could support workers by providing night lighting to facilitate their work and even powering refrigeration equipment to help preserve the catch.

Globally, the use of alternative energy sources is increasing. Recent data suggests that the economic gap between fossil fuel-generated energy and renewable energy is narrowing.

Wave energy has emerged as a competitive source and has caught up with more established technologies. However, it requires assessment of its social and environmental impacts. Despite this, it has a promising

future, making it an attractive option for coastal countries.

### 5. Conclusions

The presented research demonstrates the feasibility of implementing wave technology farms on the southwest coast of Baja California, Mexico. Additionally, the research provides a method for assessing the levelized cost of energy (LCOE) from a wave energy converter (WEC) farm perspective. This includes selecting optimal areas within a study site and determining the best distribution of devices to achieve the highest installed capacity.

The study analysed the use of Wave Dragon and Archimedes Wave Swing devices. The latter was found to have a better cost/production ratio. Farm E, located between UTM coordinates 520230 E, 3524036 N; and 520710 E, 3525656 N, had the lowest generation cost of 0.10 USD \$2022/kWh.

However, Farm E, located between UTM coordinates 520530 E, 3524606 N; and 521070 E, 3525956 N, had the lowest generation cost of 0.30 USD\$2022/kWh among the Wave Dragon farms. This indicates that the use of this device is currently not feasible due to its low energy production in relation to the area it occupies. Using a larger number of devices, specifically Archimedes Wave Swing, in the area occupied by Wave Dragons is a more feasible option.

The proposed farms are situated within 10 km of the fishing port of El Sauzal and offer a viable solution for electricity supply, contributing to the existing energy matrix of the area. At the same time, the installed devices can absorb part of the energy of offshore waves, helping to prevent possible erosion of the surrounding coastline. This provides a sustainable solution to current needs. It is important to use subject-specific vocabulary when it conveys the meaning more precisely than a similar non-technical term.

The sensitivity analysis revealed that the farm’s location has an exponential impact on the LCOE. In summary, if the site is unsuitable, the cost will increase significantly. However, if the site requires all the capabilities of the device, the impact will be less severe. Therefore, it can be concluded that a site requiring the maximum number of WECs is not necessary to achieve competitive generation costs. Additionally, the analysis demonstrates that unit efficiency has a significant impact on LCOE. This is due to the fact that higher efficiency leads to a higher CF, resulting in a lower generation cost.

Finally, the study found that the steel price, debt/equity structure, and shared use factor have little impact on the LCOE value. Therefore, it can be concluded that economic variables of the project can be flexible without affecting the final cost of generation.

Almost all feasibility assessments, including the one conducted here, are limited by the quality and quantity of available information on prices, debt costs, and taxes due to the absence of associated industry data. However, the presented methodology may be useful for more accurate decision-making. Additionally, the sensitivity analysis is helpful in defining trends, although the numerical values may change significantly due to economic and political factors.

### Data availability

The data produced and analysed in this research is available upon request.

### CRedit authorship contribution statement

**Alfredo Sánchez:** Writing – original draft, Visualization, Methodology, Investigation, Conceptualization. **Edgar Mendoza:** Writing – review & editing, Validation, Methodology, Formal analysis, Conceptualization.

## Declaration of competing interest

The authors declare that they have no known competing financial interests or personal relationships that could have appeared to influence the work reported in this paper.

## References

- [1] IRENA, Global Energy Transformation: A Roadmap to 2050, International Renewable Energy Agency, Abu Dhabi, 2018.
- [2] M. Melikoglu, Current status and future of ocean energy sources: a global review, *Ocean Eng.* 148 (2018) 563–573.
- [3] G. Chang, C.A. Jones, J.D. Roberts, V.S. Neary, A comprehensive evaluation of factors affecting the levelized cost of wave energy conversion projects, *Renew. Energy* 127 (2018) 344–354.
- [4] E. Amini, H. Mehdipour, E. Faraggiana, D. Golbaz, S. Mozaffari, G. Bracco, M. Neshat, Optimization of hydraulic power take-off system settings for point absorber wave energy converter, *Renew. Energy* 194 (2022) 938–954.
- [5] C. Guo, W. Sheng, D.G. De Silva, G. Aggidis, A review of the levelized cost of wave energy based on a techno-economic model, *Energies* 16 (5) (2023) 2144.
- [6] M.M. Vanegas-Cantarero, S. Pennock, T. Bloise-Thomaz, H. Jeffrey, M.J. Dickson, Beyond LCOE: a multi-criteria evaluation framework for offshore renewable energy projects, *Renew. Sustain. Energy Rev.* 161 (2022) 112307.
- [7] L. Wang, T. Zhao, M. Lin, H. Li, Towards realistic power performance and techno-economic performance of wave power farms: the impact of control strategies and wave climates, *Ocean Eng.* 248 (2022) 110754.
- [8] R. O'Connell, M. Kamidelvand, R. Furlong, M. Guerrini, M. Cullinane, J. Murphy, An advanced geospatial assessment of the Levelised cost of energy (LCOE) for wave farms in Irish and western UK waters, *Renew. Energy* 221 (2024) 119864.
- [9] P. Ruiz-Minguela, D.R. Noble, V. Nava, S. Pennock, J.M. Blanco, H. Jeffrey, Estimating future costs of emerging wave energy technologies, *Sustainability* 15 (1) (2023) 215.
- [10] P. Salles, R. Silva, Infraestructura de protección costera, in: E. Rivera Arriaga, G. J. Villalobos, I. Azuz Adeath, y F. Rosado May (Eds.), *El Manejo Costero en Mexico*, Universidad Autónoma de Campeche, SEMARNAT, CETYS-Universidad, Universidad de Quintana Roo, 2004, pp. 179–190.
- [11] Municipio de Ensenada. <http://www.inafed.gob.mx/work/enciclopedia/EMM02/bajacalifornia/municipios/02001a.html>. (accessed Mar. 20, 2022).
- [12] C. Beels, P. Troch, K. Visch, G. de Backer, J. Rouck, J. Kofoed, Numerical simulation of Wake effects in the lee of a farm of wave dragon wave energy converters, in: *Proceedings of the 8th European Wave and Tidal Energy Conference, EWTEC*, Uppsala, Sweden, 2009.
- [13] Wave Dragon, <http://www.wavedragon.net/specifications/> (accessed Feb. 15, 2022).
- [14] N. Guillou, G. Chapalain, Annual and seasonal variabilities in the performances of wave energy converters, *Energy* 165 (2018) 812–823, 2018.
- [15] J.M.B.P. Cruz, A.J.N.A. Sarmiento, Sea state characterisation of the test site of an offshore wave energy plant, *Ocean Eng.* 34 (5–6) (2006) 763–775.
- [16] M. Prado, H. Polinder, Case study of the Archimedes Wave Swing (AWS) direct drive wave energy pilot plant, in: M. Mueller, H. Polinder (Eds.), *Woodhead Publishing Series in Energy, Electrical Drives for Direct Drive Renewable Energy Systems*, Woodhead Publishing, 2013, pp. 195–218.
- [17] S. Diaconu, E. Rusu, Evaluation of various WEC devices in the Romanian near shore, in: *WSEAS International Conference on Energy and Environment Technologies and Equipment (EEETE)*, 2013. Brasov, Romania.
- [18] H. Hershbach, B. Bell, P. Berrisford, G. Biavati, A. Horányi, J. Muñoz Sabater, J. Nicolas, C. Peubey, R. Radu, I. Rozum, D. Schepers, A. Simmons, C. Soci, D. Dee, J.-N. Thépaut, ERA5 hourly data on single levels from 1940 to present, Copernicus Climate Change Service (C3S) Climate Data Store (CDS) (2023), 01-Aug-2021.
- [19] R. Silva, A.G.L. Borthwick, R.E. Taylor, Numerical implementation of the harmonic modified mild-slope equation, *Coast Eng.* 52 (5) (2005) 391–407.
- [20] R. Silva, WAPO - Manual de usuario y guía de referencia, UNAM, 2010.
- [21] E. Mendoza, R. Silva, B. Zannutigh, B. Angelelli, T. Lykke-Andersen, L. Martinelli, J.Q. Hark-Nørgaard, P. Ruol, Beach response to wave energy converter farms acting as coastal defence, *Coast Eng.* 87 (2014) 97–111.
- [22] J.Q. Hark-Nørgaard, T.L. Lykke-Andersen, Investigation of wave transmission from a floating wave dragon wave energy converter, in: *Proceedings of the Twenty-Second International Offshore and Polar Engineering Conference*, Rhodes, Greece, 2012.
- [23] X.L. Zhao, D.Z. Ning, Q.P. Zou, D.S. Qiao, S.Q. Cai, Hybrid floating breakwater-WEC system: a review, *Ocean Eng.* 186 (2019) 106126.
- [24] J.V. Hernández-Fontes, M.L. Martínez, A. Wojtarowski, J.L. González-Mendoza, R. Landgrave, R. Silva, Is ocean energy an alternative in developing regions? A case study in Michoacan, Mexico, *J. Clean. Prod.* 266 (2020) 121984.
- [25] Artículo 9 Determinación del ISR del ejercicio. <https://www.sat.gob.mx/articulo/93578/articulo-9> (accessed Oct. 20, 2021).
- [26] Ley del Impuesto sobre la renta, 2021.
- [27] Banco de México. <https://www.banxico.org.mx/SielInternet/consultarDirectorioInternetAction.do?accion=consultarCuadro&idCuadro=CI34&sector=18&locale=es> (accessed Feb. 10, 2022).
- [28] Invenómica <https://www.invenomica.com.ar/riesgo-pais-emi-america-latina-serie-historica/> (accessed Feb. 05, 2022).
- [29] Damodaran. [http://people.stern.nyu.edu/adamodar/New\\_Home\\_Page/dataarchive/d.html](http://people.stern.nyu.edu/adamodar/New_Home_Page/dataarchive/d.html) (accessed Feb. 20, 2022).
- [30] J.P. Kofoed, P. Frigaard, E. Friis-Madsen, H.C. Sørensen, Prototype testing of the wave energy converter wave dragon, *Renew. Energy* 31 (2) (2006) 181–189.
- [31] Trading Economics. <https://tradingeconomics.com/commodity/steel> (accessed Mar. 01, 2022).
- [32] G.J. Dalton, R. Alcorn, T. Lewis, Case study feasibility analysis of the Pelamis wave energy converter in Ireland, Portugal and North America, *Renew. Energy* 35 (2) (2010) 443–455.
- [33] S. Fernández, L. Otero, A. Rodríguez, Estimación de la capacidad de endeudamiento del proyecto: propuesta de un modelo de cobertura temporal, La gestión de la diversidad: XIII Congreso Nacional, IX Congreso Hispano-francés, Logroño (La Rioja) 1 (1999) 761–772.
- [34] EIA, Levelized Cost of New Generation Resources in the Annual Energy Outlook 2013, US Energy Information and Administration, 2013, pp. 1–5. January.
- [35] J.V. Hernández-Fontes, A. Felix, E. Mendoza, Y. Rodríguez, R. Silva, On the marine energy resources of Mexico, *J. Mar. Sci. Eng.* 7 (6) (2019) 191.
- [36] E. Gorr-Pozzi, H. García-Nava, F. García-Vega, J.A. Zertuche-González, Techno-economic feasibility of marine eco-parks driven by wave energy: a case study at the coastal arid region of Mexico, *Energy for Sustainable Development* 76 (2023) 101299.
- [37] CENACE. <https://www.cenace.gob.mx/Paginas/Publicas/Info/DemandaRegional.aspx> (accessed Apr. 13, 2022).